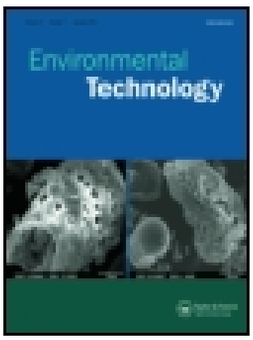

Environmental Technology

ISSN: (Print) (Online) Journal homepage: https://www.tandfonline.com/loi/tent20

Influence of modulus of alkaline activator on the removal of Pb^{2+} by mesoporous geopolymer adsorbent

Tian Lan, Pinfang Li, Xiangling Li, Jingting Guo, Qian Huang, JianJian Geng, Qingjie Zhao, Wei Yang & Shiwen Guo

To cite this article: Tian Lan, Pinfang Li, Xiangling Li, Jingting Guo, Qian Huang, JianJian Geng, Qingjie Zhao, Wei Yang & Shiwen Guo (2021): Influence of modulus of alkaline activator on the removal of Pb^{2+} by mesoporous geopolymer adsorbent, Environmental Technology, DOI: 10.1080/09593330.2021.1946597

To link to this article: https://doi.org/10.1080/09593330.2021.1946597

Published online: 22 Jul 2021.

Submit your article to this journal

Article views: 29

View related articles

View Crossmark data

Full Terms & Conditions of access and use can be found at
https://www.tandfonline.com/action/journalInformation?journalCode=tent20

ENVIRONMENTAL TECHNOLOGY
https://doi.org/10.1080/09593330.2021.1946597

Taylor & Francis
Taylor & Francis Group

Check for updates

Influence of modulus of alkaline activator on the removal of Pb^{2+} by mesoporous geopolymer adsorbent

Tian Lan[b,e], Pinfang Li[b], Xiangling Li[b], Jingting Guo[c], Qian Huang[a,g], JianJian Geng[d], Qingjie Zhao[f], Wei Yang[b] and Shiwen Guo[a]

[a]College of Resources and Environmental Sciences, China Agricultural University, Beijing, People's Republic of China; [b]College of Land Science and Technology, China Agricultural University, Beijing, People's Republic of China; [c]Beijing Environmental Engineering Technology Co., Ltd, Beijing, People's Republic of China; [d]Yunnan Institute of Tropical Crops, Jinghong, Yunnan, People's Republic of China; [e]School of Environment, Tsinghua University, Beijing, People's Republic of China; [f]College of Forestry, Hainan University, Haikou, People's Republic of China; [g]Zhejiang Allianz Testing Technology Service Co., Ltd, Hangzhou People's Republic of China

ABSTRACT

In this study, we synthesised metakaolin-based mesoporous geopolymer adsorbent and investigated the effect of alkaline activator modulus (molar ratios of SiO_2/Na_2O) on Pb^{2+} adsorption. The geopolymer prepared using 1.2 M alkaline activator performs excellent Pb^{2+} removal with a maximum adsorption capacity of 172.71 mg g^{-1}. The pseudo-second-order model fit the adsorption kinetics satisfactorily, indicating that the adsorption process is dominated by chemical adsorption. The adsorption data appropriately fit the Langmuir isotherm model. The contributions of adsorption methods corresponding to the total quantity adsorbed declined in the following order: EDTA extraction (formation of Pb aluminium oxide and Pb-containing amorphous materials) > residual fraction (Pb stabilisation in the tetrahedral aluminosilicate network) > ion exchange. Overall, the alkaline activator modulus significantly influenced the Pb^{2+} adsorption characteristics of the geopolymer adsorbent.

ARTICLE HISTORY
Received 20 January 2021
Accepted 1 June 2021

KEYWORDS
Metakaolin; geopolymerisation; adsorption performance; alkaline activator; Pb^{2+}

1. Introduction

Heavy metals are released into the environment due to mining activities; fertilizer and pesticide use; battery disposal and tannery activities and from metal plating and paper industries [1]. These water and soil contaminants can enter and accumulate in the human body through food and water and adversely impact human health [2]. Lead, one of the heavy metals, is a kind of industrial pollutant widely existing in the wastewater. Lead accumulation in the body causes cancer, anaemia, abdominal pain, muscle and joint pain, kidney problems, and high blood pressure [3]. Additionally, lead can impede plant growth and significantly inhibit plant physiological characteristics such as the height, number of roots and root length.

Considerable research has been conducted on heavy metal removal from wastewater using methods such as electrodialysis, photocatalytic technologies [4–6], ion exchange [7], chemical precipitation [8], electrochemical treatment [9], and adsorption [10]. Adsorption is an attractive removal technique; it is easy and efficient; uses inexpensive natural materials; and produces environment-friendly waste [11]. Heavy metal adsorption has been performed using various natural and artificial materials [12,13]. However, factors such as process efficiency, environmental friendliness and economic

CONTACT Shiwen Guo guosw@cau.edu.cn College of Resources and Environmental Sciences, China Agricultural University, 100193, Beijing, People's Republic of China

© 2021 Informa UK Limited, trading as Taylor & Francis Group

Table 1. Composition of MK.

Composition	SiO_2	Al_2O_3	Fe_2O_3	MgO	CaO	Na_2O	K_2O	TiO_2	P_2O_5	L.O.L
wt%	53.73	40.21	1.02	0.28	0.13	0	1.13	1.87	0.07	1.56

feasibility, limit the widespread use of heavy metal sorbents [14].

Geopolymers, with a three-dimensional structure consisting of SiO_4 and AlO_4 tetrahedra, are amorphous, inorganic gel materials that can be prepared from fly ash, clay, metakaolin (MK), raw kaolin, and slag [13]. The zeolite-like structure of geopolymers engenders useful properties such as good mechanical strength, rapid hardening and acid–alkali resistance that contribute to their widespread use in cements and as refractory materials [15]. Geopolymers have attracted attention because they are easily synthesised at room temperature with less emission of greenhouse gases (*e.g.* CO_2, SO_2, and NO_x) and can be fabricated from abundant and accessible raw materials [13,16].

Recent research indicates that geopolymers have excellent properties that assist in adsorbing heavy metals from wastewater. Al-Harahsheh synthesised fly ash-based geopolymer powders that exhibited adsorption capacities of 152 and 134 mg g^{-1} for Pb^{2+} and Cu^{2+}, respectively [17]. Al Zboon [18] discovered that the adsorption capacity of geopolymers prepared from natural volcanic tuff reached 14.8 mg g^{-1}. Cheng [19] prepared a metakaolin-based geopolymer for Pb^2, Cu^{2+}, Cr^{3+}, and Cd^{2+} removal and reported maximum adsorption capacities of 147.06, 48.78, 19.94, and 67.57 mg g^{-1}, respectively. Kara's research [16] observed that maximum monolayer adsorption capacities of Zn^{2+} and Ni^{2+} ions by metakaolin-based geopolymer was 1.14 $\times 10^{-4}$ and 7.24 $\times 10^{-3}$ mol g^{-1}, respectively.

The parameters employed in geopolymer preparation affect its adsorption capacity and other properties. Shu [20] prepared coal fly ash-based geopolymers to remove H_2SO_4 mist and discovered that the adsorbent activity varied based on the mass ratios of fly ash to activator to water. Ge [21] prepared an inorganic geopolymer membrane using metakaolin and sodium silicate solutions to remove Ni^{2+} from wastewater, and observed that the surface area decreased as the H_2O/Na_2O ratio increased. However, few reports exist on the ability of the alkaline activator conditions involved in geopolymer preparation that influence the material's capacity to adsorb heavy metals. In the present study, geopolymers were prepared under different alkaline activator conditions and the resulting differences in Pb^{2+} adsorption ability were characterised. Pb-loaded materials were extracted sequentially to study the contribution of the corresponding processes on the total quantity adsorbed. The mechanism of Pb^{2+} adsorption was investigated using SEM–EDX, FTIR, XRD and XPS.

2. Materials and methods

2.1. Materials

Metakaolin (MK) was sourced from Zhengzhou in Henan Province, China. The composition of MK is presented in Table 1. The initial modulus of sodium silicate was adjusted to 3.3 using NaOH. The alkaline activator solution (AAS) was prepared by mixing sodium silicate and sodium hydroxide at molar ratios of SiO_2/Na_2O = 0.8, 1.2, 1.6, and 2.0 and sonicated for 20 min.

2.2. Adsorbent preparation

The Metakaolin, alkaline activator solution (AAS) and distilled water were mixed (1000 rpm, 25 min) at a mass ratio of 100:80:60 (MK: AAS: distilled water) to prepare a geopolymer slurry. The product was cured for 16 days under alternating conditions of room temperature and 80 °C [22]. The resulting geopolymer block was crushed, passed through a 0.5 mm sieve, and washed with distilled water to remove excess NaOH. The terms MG-0.8, MG-1.2, MG-1.6, and MG-2.0 represent the geopolymers prepared under alkaline activator molar ratios of 0.8, 1.2, 1.6, and 2.0, respectively.

2.3. Batch-wise adsorption

The prepared adsorbent (0.100 g) was added to 25 mL aqueous $Pb(NO_3)_2$ solution. The mixture was stirred at 200 rpm and 25 °C to investigate the adsorption of Pb^{2+} by various materials. The pH of each 300 mg L^{-1} Pb^{2+} solution was adjusted to a value between 1.0 and 6.0, with either 0.01 M HNO_3 or NaOH. Kinetic experiments were performed for 0–600 min using 300 mg L^{-1} metal ion solutions at pH 3.0. Adsorption isotherms were determined by stirring solutions at pH 3.0 for 400 min with initial Pb^{2+} concentrations varying between 0 and 1000 mg L^{-1}.

2.4. Reusability study

The reusability of the synthesised geopolymers was investigated by consecutive adsorption–desorption experiments. A desorbent, Na_2EDTA was selected for

the following experiments. In each cycle, 0.5 g adsorbent was added to 100 mL of a 100 mg L^{-1} Pb^{2+} solution with a reaction time of 400 min. The collected adsorbent was transferred to 100 mL of 0.01 M EDTA-2Na and shaken at 200 rpm for 2 h. The regeneration tests were conducted five times under similar conditions to evaluate the reusability.

2.5. Pb desorption tests

Pb-loaded samples were prepared by adding 200 mg adsorbent to 30 mL Pb^{2+} solution (800 mg L^{-1}). Adsorption equilibrium was achieved by shaking the samples at 200 rpm for 10 h at 25 °C. The sequential extraction steps of heavy metals adsorbed by different methods are shown in Table 2 [22].

2.6. Material characterisation and analysis

Sample morphology was analysed using SEM (Phenom ProX, Thermo Fisher Scientific). Elemental composition was estimated by EDX. FTIR spectra were recorded by KBr disks at 400–4000 cm^{-1} using a Tensor 27 spectrometer (Bruker, Germany). XRD patterns of the samples were determined with a D8 Advance diffractometer (Bruker AXS, Germany) using Ni-filtered Cu K_α radiation at $2\theta = 5–70°$. XPS measurements were performed using an AXIS Supra spectrometer (Kratos Analytical) with Mg-K_α radiation emitted from a double anode at 50 W.

3. Results and discussion

3.1. Characterisation

Figure 1 shows electron micrographs of MK, MG-1.2, and the geopolymer with the adsorbed Pb (MG-1.2-Pb). The SEM image of MK reveals a sheet structure with particle sizes < 30 µm. Many studies have reported that geopolymerisation forms nanoparticles [23,24], but these structures were not observed in the present study. The geopolymers contain a large number of pores, which are formed due to binding of particles of < 10 µm diameters (Figure 1c and 1d). The pore size of the agglomerated structures reduced, while the roughness of the particle surfaces increased after Pb^{2+} adsorption (Figure 1e and 1f).

Table 2. Continuous extraction of heavy metal.

Abbreviation	Full name	Operation
HM_{phy}	Physical fraction	Shake 200 mg sample with 25 mL distilled water at 200 rpm for 3 h at 25°C
HM_{exc}	Exchangeable fraction	Shake the residual sample with 25 mL 1 M $MgCl_2$ solution (pH = 7) at 200 rpm for 2 h at 25 °C
HM_{EDTA}	EDTA-extractable fraction	Shake the residual sample with 25 mL 0.05 M EDTA-2Na solution at 200 rpm for 2 h at 25 °C
HM_{res}	Residual fraction	Calculated by equation: $HM_{res} = HM_{total} - HM_{phy} - HM_{exc} - HM_{EDTA}$

HM_{total}: total amount of adsorbed Pb^{2+}.

Table 3[22] shows the specific surface area and pore volume of the adsorbent. The S_{BET} of MG-0.8 and MG-1.2 are 8.16 and 16.15 m^2 g^{-1}, respectively, which are higher than the corresponding S_{BET} value of MK. Additionally, the pore volume of geopolymers is five times higher than that of the raw materials. The increase in pore volume of MK-based geopolymer is mainly due to the increase in mesopores and macropores.

The mineral phases present in the MK sample as identified by XRD patterns (Figure 2a) are aluminium silicate, mullite, and quartz [22]. The characteristic SiO_2 diffraction peak observed at 26° in all samples indicates that the geopolymer contains unreacted quartz residues. However, disappearance of the peaks at 35–55° indicates that MK dissolves under the alkaline conditions of geopolymer preparation. The environment of aluminium atom varies relatively to that of silicon during the conversion of structural MK to geopolymer, resulting in a greater degree of polymerisation [25].

Figure 2b shows the FTIR absorption spectra of the samples. The peak at 1076 cm^{-1} shifts to a lower frequency at ~1026 cm^{-1} after geopolymerisation of MK, indicating the formation of an alkaline aluminosilicate gel [26]. During polycondensation, the Si – O–T bond stretches and the bond angle decreases, which reduces the vibrational force constant [27]. Moreover, the shift may be attributed to an increase in the fraction of silicon sites bound to non-bridging oxygen atoms [28]. The typical Al^{3+} absorption band at 798 cm^{-1} in the MK sample is absent in the synthetic geopolymer [29]. However, the significant peak at 696 cm^{-1} in the geopolymer spectrum can be attributed to tetrahedral SiO_4 or AlO_4 units in the polymeric structure [30]. This result indicates a disintegration of the original octahedral structure of the raw materials during the formation of the geopolymer.

3.2. Adsorption studies

The amount of Pb adsorbed increases with increasing pH as shown in Figure 3a and 3b. The adsorption capacity at low pH is limited by the competition between H_3O^+ and Pb^{2+}. However, the amount of adsorbed metal ions increases as the pH increases and the concentration of H_3O^+ decreases [31]. The equilibrium pH values do not

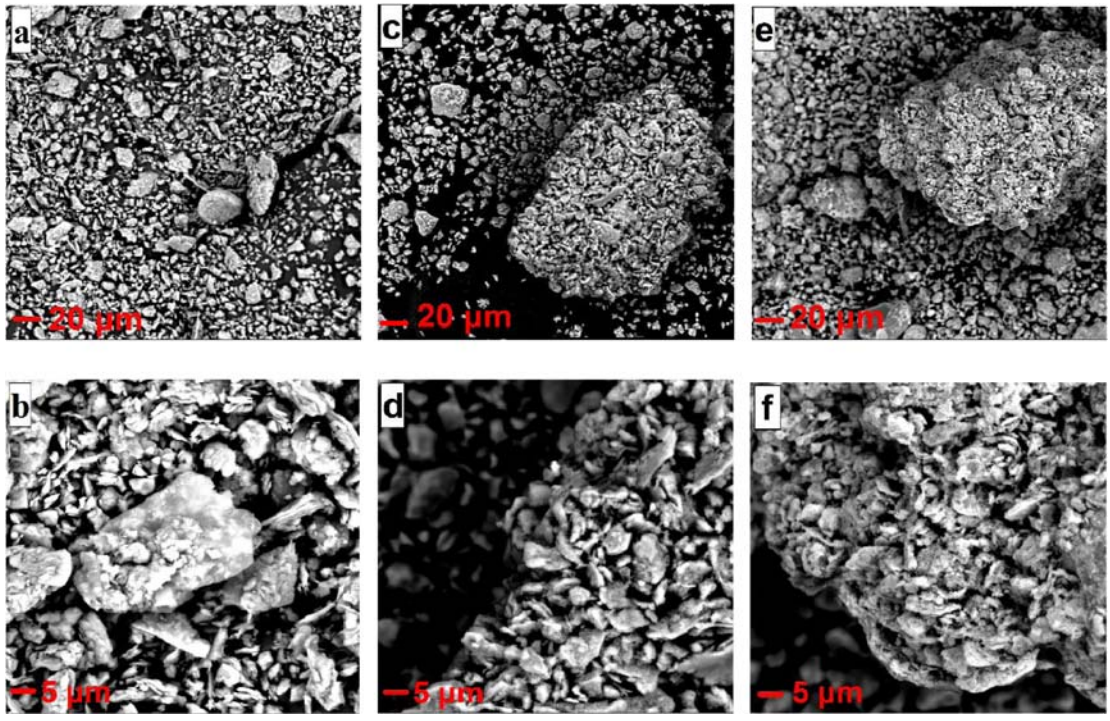

Figure 1. SEM micrographs of (a, b) MK, (c, d) MG-1.2, and (e, f) MG-1.2-Pb at the indicated magnifications.

increase significantly when the initial pH is > 3. This may be due to the surface precipitation of Pb^{2+} and OH^{-} as the pH increases above 6 [32]. Therefore, pH 3.0 is optimal for the subsequent adsorption experiments.

As shown in Figure 3c and 3d, Pb^{2+} adsorption on the geopolymer increases with increasing contact time, peaks after 300 min, and remains constant thereafter. Significant removal of Pb^{2+} (86.9%) occurs within the first 40 min for MK, with only slight variations observed after 120 min. Thus, a 300 min mixing time is sufficient to achieve the adsorption equilibrium. The contact time in subsequent experiments was set to 400 min to shorten the processing time, ensuring that sufficient time was provided to attain adsorption equilibrium. Adsorption kinetics were analysed by pseudo-first-order and pseudo-second-order models to investigate the adsorption mechanism of Pb^{2+} on the geopolymers and MK [33,34].

$$\ln(q_e - q_t) = \ln q_e - k_1 t \quad (1)$$

$$\frac{t}{q_t} = \frac{1}{k_2 q_e^2} + \frac{t}{q_e} \quad (2)$$

where q_t and q_e are the quantities of Pb^{2+} adsorbed (mg g^{-1}) at equilibrium and at contact time t (min), respectively, and k_1 (min^{-1}) and k_2 (g (mg $min^{-1})^{-1}$) are rate constants.

The resulting fitted values are shown in Table 4. The pseudo-second-order model showed a better fit to the experimental data. Hence, the process may involve chemical adsorption accompanied by electron exchange or sharing [35,36].

The maximum quantities of Pb^{2+} adsorbed by MK, MG-0.8, MG-1.2, MG-1.6, and MG-2.0 were 16.53, 134.34, 172.71, 162.76, and 79.19 mg g^{-1}, respectively (Figure 2c and 2d). The conversion of MK to a geopolymer increased the amount of Pb^{2+} adsorbed by factors of 4.8–8.1. Previous research indicated that MG-0.8 exhibited the maximum capacity for Cd^{2+} adsorption [22]. However, the geopolymer prepared using 1.2 M alkali activator modulus has the maximum capacity for Pb^{2+} removal from the solution. This observation suggests that differences exist in the mechanisms of Pb^{2+} and Cd^{2+} adsorption by geopolymers. According to GB 5749-2006 [37] and GB 8978-1996[38], the concentration limits of Pb^{2+} in drinking water and wastewater are 0.01 mg L^{-1} and 1.0 mg L^{-1}, respectively. When the initial concentration of the solution is low, the absorbent used in this study can ensure that the Pb content is within the wastewater discharge standard.

Table 3. BET specific surface area and pore volume of samples [22].

Sample	S_{BET} (m^2 g^{-1})	Pore volume (mL g^{-1})	Pore volume (ml g^{-1})		
			< 2 nm	2–50 nm	> 50 nm
MK	2.54	0.004	0	0.0028	0.0012
MG-0.8	8.16	0.021	0	0.0151	0.0059
MG-1.2	16.05	0.034	0	0.0208	0.0132

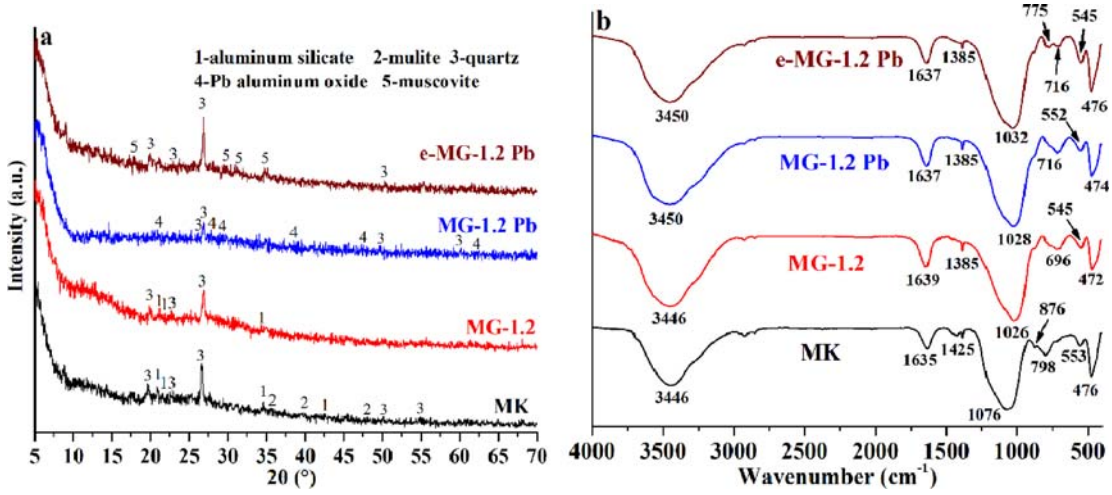

Figure 2. (a) XRD patterns and (b) FTIR spectra of MK, MG-1.2, MG-1.2-Pb, and e-MG-1.2-Pb (EDTA-extractable MG-1.2-Pb).

The Langmuir Equation (4) and Freundlich Equation (5) models are commonly used to describe the interaction between the adsorbents and the metal ions:

$$q_e = \frac{K_L q_m C_e}{1 + K_L C_e} \tag{3}$$

$$q_e = K_F C_e^{\frac{1}{n}} \tag{4}$$

where q_e (mg g^{-1}) and q_m are the adsorption capacity at equilibrium and the maximum adsorption capacity, respectively; C_e (mg L^{-1}) is the equilibrium concentration of Pb^{2+}; K_L (L mg^{-1}) is the Langmuir constant that relates to the free energy and adsorption affinity; and K_F and n are Freundlich constants related to the adsorption capacity and adsorption intensity, respectively.

The R^2 value of the Langmuir isotherm model for MG-0.8, MG-1.2, and MK was greater than the corresponding R^2 values of the Freundlich isotherm (Table 4). However, the R^2 value of the Langmuir isotherm for MG-1.6 and MG-2.0 was less compared to the R^2 value of the Freundlich isotherm. The fitting results indicated that monolayer adsorption prevails in the adsorption of Pb^{2+} by MG-0.8, MG-1.2, and MK. However, Pb^{2+} adsorption by MG-1.6 and MG-2.0 adsorbents most likely proceeds as multilayer adsorption [31,32]. The Freundlich isotherm R^2 value for MG-0.8, MG-1.2, and MK was close to 1, and the value of 1/n (0.22–0.67) was less than 1, indicating strong adsorption with heterogeneous characteristics [39].

3.3. Adsorption mechanism

3.3.1. Chemical speciation of adsorbed Pb

Figure 4 shows the distribution of the adsorbed forms in the Pb-loaded samples. The contributions of physically adsorbed, ion-exchangeable, EDTA-extractable and residual fractions in Pb-loaded MK were 0.20, 2.21, 1.28, and 9.79 mg g^{-1}, respectively. For geopolymers, the amount of physically adsorbed Pb^{2+} was negligible, which was less than 0.15% of the total adsorption capacity. The contribution of ion-exchangeable Pb^{2+} in MG-0.8, MG-1.2, and MG-1.6 did not exceed 1.3%, whereas it was 10.09% in MG-2.0. The EDTA-extractable Pb^{2+} in the geopolymer samples ranged between 32.69–83.48 mg g^{-1}, which considerably surpassed the quantity in MK. The residual Pb content in MG-0.8, MG-1.2, and MG-1.6 ranged between 35.27–45.10 mg g^{-1} and accounted for 30.67 – 37.49% of the total adsorbed content. The residual Pb content in MG-2.0 was 13.05 mg g^{-1}, which was slightly greater than that in MK. The above results indicate that, after MK-to-geopolymer conversion, a significant increase in Pb^{2+} adsorption occurs in the EDTA-extractable form, followed by the residual fraction.

3.3.2. EDX analysis

The EDX (Figure 5) results indicate that O, Si, Al, and Na were the major components of the geopolymer structure. The sodium distribution on the sample surface is remarkably similar to those of the aluminium and silicon distributions. Free and exchangeable Na^+ ions present on the geopolymer surface before adsorption are replaced by Pb^{2+} after adsorption. The Na observed after adsorption is therefore fixed in the aluminosilicate lattice [40]. The brightness and outline of the Pb responses strongly correspond to the positions of O, Al, Si, and Na reflecting a high degree of spatial correlation between the adsorbed Pb and the underlying elements.

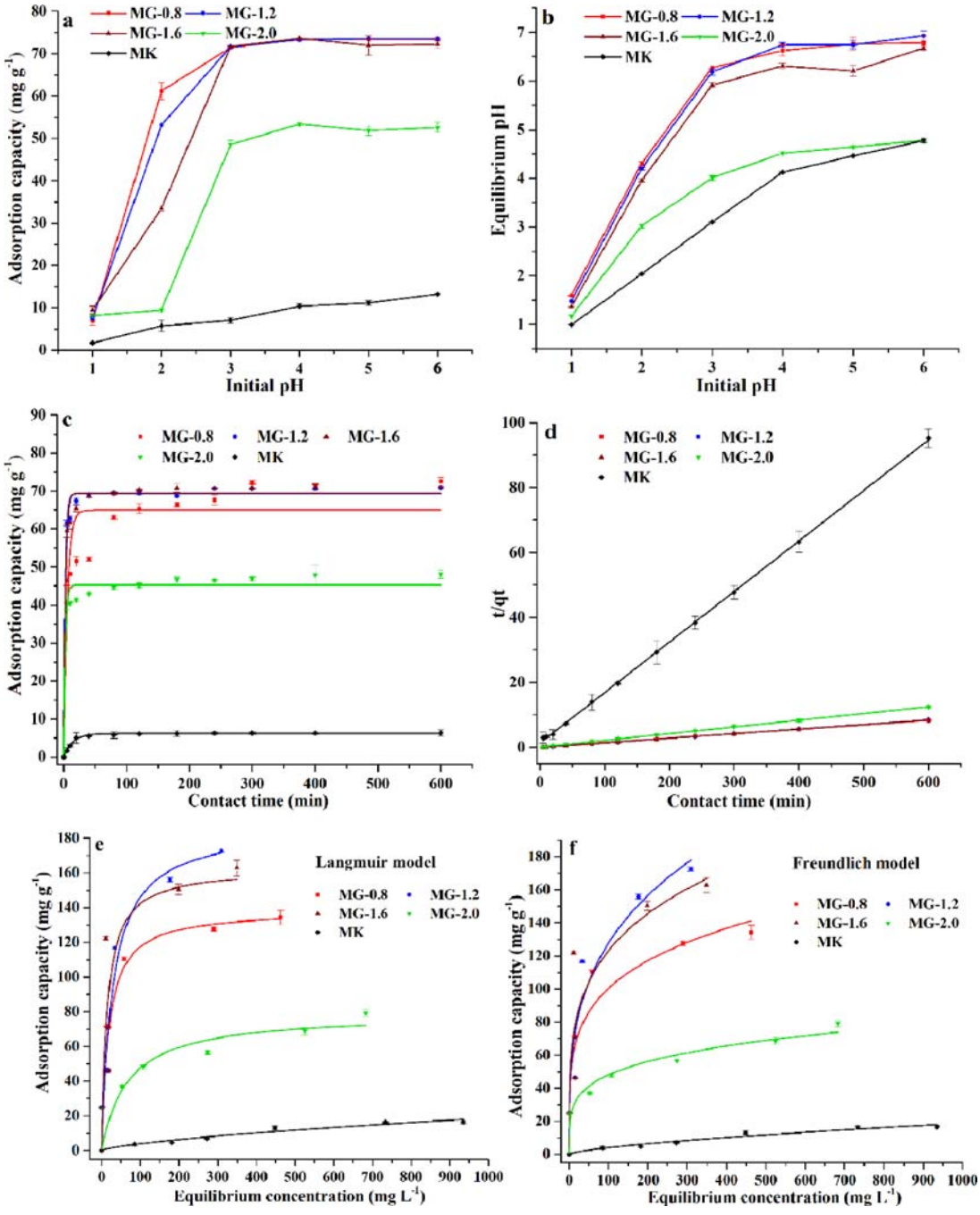

Figure 3. Adsorption characteristics of MK and geopolymers: (a, b) effect of initial pH on Pb^{2+} adsorption, (c) pseudo-first-order kinetic model of adsorption (effect of contact time), (d) pseudo-second-order kinetic model of adsorption (effect of contact time), and (e, f) effect of initial Pb^{2+} concentration on adsorption isotherms.

3.3.3. Total survey of XPS spectra

The complete and high-resolution XPS spectra of MG-1.2, MG-1.2-Pb, and e-MG-1.2-Pb (EDTA-extractable MG-1.2-Pb) are shown in Figure 6. The principal Al 2p, Si 2p, O 1s, Na 1s, and C 1s peaks are observed in MG-1.2, MG-1.2-Pb, and e-MG-1.2-Pb. The MG-1.2-Pb sample shows distinct peaks at binding energies of ~139 and 144 eV, indicating that Pb^{2+} is adsorbed by the geopolymer. The Na 1s peak does not change despite Pb^{2+} adsorption, which indicates that the principal form of adsorbed material in the geopolymer is not exchangeable, but rather fixed in the aluminosilicate network. This result is consistent with the SEM-EDX result (Figure 5). The extraction of Pb-loaded geopolymer with EDTA, significantly decreases the intensities of the Pb XPS peaks at 139 and 144 eV. This indicates that a substantial amount of adsorbed Pb is soluble in EDTA, which is consistent with the

Table 4. Kinetic parameters, adsorption isotherm constants for Pb^{2+} adsorption on geopolymers and MK.

			Materials				
Categories	parameter	Units	MK	MG-0.8	MG-1.2	MG-1.6	MG-2.0
Pesudo-first-order model	q_e	mg g^{-1}	6.15	64.92	69.25	69.4	45.26
	k_1	10^{-3} min^{-1}	0.069	0.178	0.406	0.352	0.398
	R^2		0.989	0.874	0.990	0.985	0.969
Pesudo-first-order model	q_e	mg g^{-1}	6.43	73.36	71.05	71.19	48.26
	k_2	10^{-4} g mg^{-1} min^{-1}	17.82	1.22	7.64	9.87	4.19
	R^2		0.997	0.990	0.994	0.994	0.998
Langmuir isotherm constants	q_{max}	mg g^{-1}	34.14	138.57	187.01	162.61	79.29
	K_l	L mg g^{-1}	0.001	0.055	0.036	0.070	0.015
	R2		0.970	0.944	0.954	0.808	0.851
Freundlich isotherm constants	K_f		0.18	35.99	33.15	40.42	17.10
	1/n		0.67	0.22	0.29	0.24	0.22
	R^2		0.959	0.939	0.943	0.844	0.974

sequential desorption results (Figure 4). The Na 1s XPS peak is enhanced in the process, indicating that the adsorption site occupied by EDTA-extractable Pb^{2+} is replaced by Na^+ from the EDTA solution. The characteristic Pb 4f peak still observed in e-MG-1.2-Pb, indicating that the adsorbed Pb cannot be completely extracted by EDTA. This material is the residual Pb fraction described in the sequential desorption study (Figure 4).

3.3.4. XRD Analysis

The adsorption mechanism was investigated using the XRD patterns of MG-1.2-Pb and e-MG-1.2-Pb. Pb aluminium oxide diffraction peaks appear in the geopolymer after Pb^{2+} adsorption (Figure 2a). Additionally, the aluminium silicate peak disappears, and the quartz peak decreases significantly. Presumably, aluminium silicate and quartz react with Pb^{2+} to form an amorphous material. The diffraction peak of lead oxide disappears after the Pb-loaded geopolymer is extracted with EDTA, suggesting the removal of Pb aluminium oxide fraction during this process.

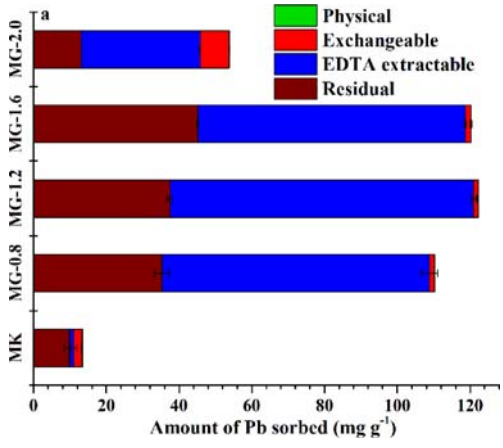

Figure 4. Loaded forms of Pb^{2+} in geopolymers and MK.

3.3.5. FTIR analysis

Figure 2b shows that after the Pb-loaded geopolymer is extracted by EDTA, the peak at 1026 cm^{-1} shifts to 1032 cm^{-1}, indicating a small variation in the Si – O–T structure. This result is consistent with the appearance of the muscovite crystals detected in the XRD studies. The FTIR band at 694 cm^{-1} is displaced to 716 cm^{-1} after the geopolymer adsorbs Pb^{2+}, indicating the involvement of tetrahedral Si or Al in the adsorption reaction. This peak does not shift after the Pb-loaded geopolymer is extracted with EDTA, suggesting the stabilisation of the tetrahedral Si or Al structure by Pb fixation. The FTIR peaks at ~476 and 545 cm^{-1} correspond to Si – O –Si bending and Si – O–Al stretching, respectively [41]. The Si – O–Al stretching peak shifts during geopolymerisation, Pb^{2+} adsorption, and EDTA desorption, indicating that the Pb^{2+} adsorbed by the Si – O–Al bond is in an EDTA-extractable state. This fraction may correspond to Pb aluminium oxide (Figure 2a).

3.3.6. Conceptual model of adsorption mechanisms

The conceptual model of the Pb adsorption mechanisms by geopolymers is divided into three parts: (1)

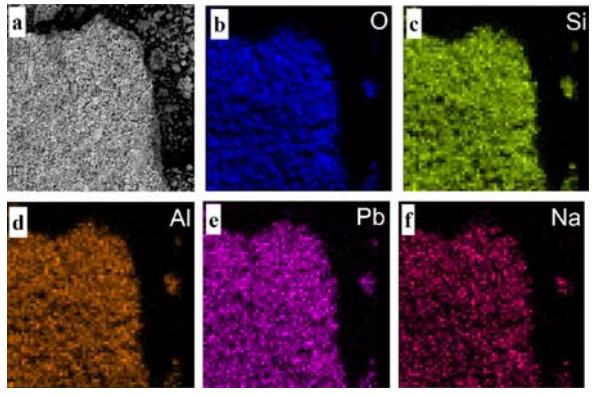

Figure 5. (a) SEM image and (b, c, d, e, f) EDS elemental dot maps of Pb-loaded MG-1.2.

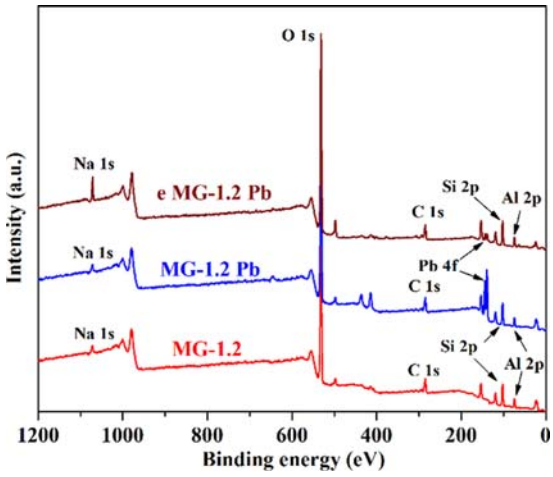

Figure 6. High-resolution XPS spectra of MG-1.2, MG-1.2-Pb, and e-MG-1.2-Pb.

cation exchange, where Pb^{2+} is exchanged with metal cations that contributes only slightly to the total adsorbed content, (2) EDTA extraction, where Pb aluminium oxide and Pb-containing amorphous materials involving Pb and Si – O–Al bonds are formed, and (3) a residual fraction, where Pb is stabilised within the tetrahedral aluminosilicate network. The Cd^{2+}-binding pathway of HM_{EDTA} involves only surface complexation via hydroxyl functional groups [42]. However, the Pb^{2+} binding modes of HM_{EDTA} are more diverse, which confirms the differences between the adsorption mechanisms of Pb^{2+} and Cd^{2+} by metakaolin-based geopolymers. The optimal molar ratio of the alkaline activator solution varies for Pb and Cd adsorption. This is mainly related to the difference in the morphology of HM_{EDTA}.

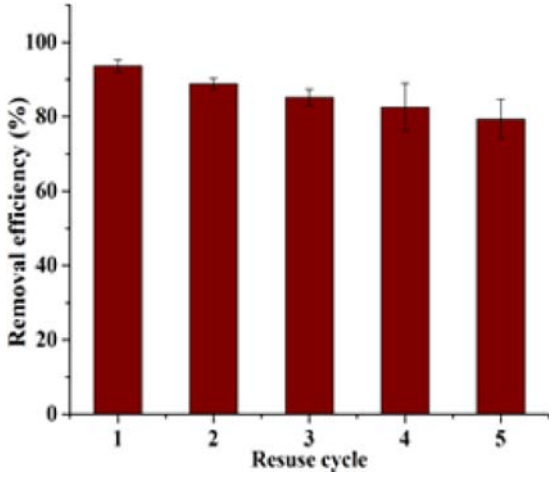

Figure 7. Pb^{2+} adsorption capacity of MG-1.2 during five consecutive adsorption–desorption cycles.

3.4. Reusability

Figure 7 presents the removal effect of Pb^{2+} by MG-1.2 adsorbent, after utilising it successively for five times. Despite the uninterrupted usage of the adsorbent five times, the removal efficiency of heavy metals remained above 79%. Therefore, geopolymer adsorbents can be effectively recycled to remove Pb.

4. Conclusions

This study observed that changes in the alkaline activator modulus (molar ratios of SiO_2/Na_2O) of geopolymer adsorbents affect their ability to adsorb Pb^{2+}. Geopolymers prepared using an alkaline activator with a modulus of 1.2 M exhibit maximum adsorption for Pb^{2+} (172.71 mg g^{-1}). Isothermal adsorption model and adsorption kinetic experiments indicate that (1) Pb^{2+} adsorption by geopolymers is dominated by chemical adsorption, (2) monolayer adsorption predominates the adsorption of Pb^{2+} by MG-0.8, MG-1.2, and MK, and (3) Pb^{2+} adsorption by MG-1.6 and MG-2.0 probably proceeds by multilayer adsorption. The contributions to Pb^{2+} adsorption in Pb-loaded geopolymers decrease in the following order: EDTA extraction > residual fraction > cation exchange. Overall, MK-based geopolymers are effective materials for wastewater purification, featuring inexpensive preparation, low energy consumption, and highly efficient Pb^{2+} adsorption.

Data availability statement

All data, models, or code generated or used during the study are available from the corresponding author by request.

Acknowledgements

We thank Tingyu Bai from the Spice and Beverage Research Institute, Chinese Academy of Tropical Agricultural Sciences guidance on the operation of SEM-EDX.

Disclosure statement

No potential conflict of interest was reported by the author(s).

Funding

This work was supported by the National Natural Science Foundation of China (NSFC, No. 51978659).

References

[1] Azimi A, Azari A, Rezakazemi M, et al. Removal of heavy metals from industrial wastewaters: a review. Chem Bio Eng Rev. 2017;4:37–59.

[2] Ren X, Zeng G, Tang L, et al. Sorption, transport and biodegradation-An insight into bioavailability of persistent organic pollutants in soil. Sci Total Environ. 2018;610:1154–1163.
[3] Zare EN, Motahari A, Sillanpää M. Nanoadsorbents based on conducting polymer nanocomposites with main focus on polyaniline and its derivatives for removal of heavy metal ions/dyes: a review. Environ Res. 2018;162:173–195.
[4] Gong J, Li Y, Zhao Y, et al. Metal-free polymeric $(SCN)_n$ photocatalyst with adjustable bandgap for efficient organic pollutants degradation and Cr(VI) reduction under visible-light irradiation[J]. Chem Eng J. 2020;402:126147.
[5] Meng X, Zhang G, Li N. $Bi_{24}Ga_2O_{39}$ for visible light photocatalytic reduction of Cr(VI): controlled synthesis, facet-dependent activity and DFT study[J]. Chem Eng J. 2017;314:249–256.
[6] Li J, Xiao C, Wang K, et al. Enhanced generation of reactive oxygen species under visible light irradiation by adjusting the exposed facet of $FeWO_4$ Nanosheets to activate oxalic acid for organic pollutant removal and Cr(VI) reduction. Environ Sci Technol. 2019;53(18):11023–11030.
[7] Bezzina JP, Ruder LR, Dawson R, et al. Ion exchange removal of Cu (II), Fe(II), Pb(II) and Zn(II) from acid extracted sewage sludge - Resin screening in weak acid media. Water Res. 2019;158:257–267.
[8] Rasaki SA, Thomas T, Yang M. Co-precipitation strategy for engineering pHtolerant and durable ZnO@MgO nanospheres for effcient, room-temperature, chemisorptive removal of Pb(II) from water. J. Environ. Chem. Eng. 2019;7(2):103019.
[9] Munoz-Morales M, Saez C, Canizares P, et al. A new strategy for the electrolytic removal of organics based on adsorption onto granular activated carbon. Electrochem. Commun. 2018;90:47–50.
[10] Yu W, Yuan P, Liu D, et al. Facile preparation of hierarchically porous diatomite/MFI-type zeolite composites and their performance of benzene adsorption: the effects of NaOH etching pretreatment. J. Hazard. Mater. 2015;285:173–181.
[11] Siyal AA, Shamsuddin MR, Khan MI, et al. A review on geopolymers as emerging materials for the adsorption of heavy metals and dyes. J Environ Manage. 2018;224:327–339.
[12] Badawi MA, Negm NA, Abou Kana MTH, et al. Adsorption of aluminum and lead from wastewater by chitosan-tannic acid modified biopolymers: isotherms, kinetics, thermodynamics and process mechanism. Int J Biol Macromol. 2017;99:465–476.
[13] Sudagar A, Andrejkovičová S, Patinha C, et al. A novel study on the influence of cork waste residue on metakaolin-zeolite based geopolymers. Appl Clay Sci. 2018;152:196–210.
[14] Blackburn RS. Natural polysaccharides and their interactions with Dye molecules: applications in effluent treatment. Environ Sci Technol. 2004;38:4905–4909.
[15] Zhou W, Yan C, Duan P, et al. A comparative study of high and lowAl_2O_3 fly ash based-geopolymers: The role of mix proportion factors and curing temperature. Mater Des. 2016;95:63–74.
[16] Amin N, Faisal M, Muhammad K, et al. Synthesis and characterization of geopolymer from bagasse bottom ash, waste of sugar industries and naturally available China clay. J Clean Prod. 2016;129:491–495.
[17] Al-Harahsheh MS, Zboon KA, Al-Makhadmeh L, et al. Fly ash based geopolymer for heavy metal removal: A case study on copper removal. J Environ Chem Eng. 2015;3(3):1669–1677.
[18] Al-Zboon K, Al-Harahsheh MS, Hani FB. Fly ash-based geopolymer for Pb removal from aqueous solution. J Hazard Mater. 2011;188:414–421.
[19] Cheng TW, Lee ML, Ko MS, et al. The heavy metal adsorption characteristics on metakaolin-based geopolymer. Appl Clay Sci. 2012;56:90–96.
[20] Shu Y, Wei X, Fang Y, et al. Removal of sulfuric acid mist from lead-acid battery plants by coal fly ash-based sorbents. J Hazard Mater. 2015;286:517–524.
[21] Ge Y, Yuan Y, Wang K, et al. Preparation of geopolymer-based inorganic membrane for removing Ni^{2+} from wastewater. J Hazard Mater. 2015;299:711–718.
[22] Lan T, Li P, Rehman F, et al. Efficient adsorption of Cd^{2+} from aqueous solution using metakaolin geopolymers. Environ Sci Pollut R. 2019;26:33555–33567.
[23] Luukkonen T, Runtti H, Niskanen M, et al. Simultaneous removal of Ni(II), As(III), and Sb(III) from spiked mine effluent with metakaolin and blast-furnace-slag geopolymers. J Environ Manage. 2016;166:579–588.
[24] Singhal A, Gangwar BP, Gayathry JM. CTAB modified large surface area nanoporous geopolymer with high adsorption capacity for copper ion removal. Appl Clay Sci. 2017;150:106–114.
[25] Wang M, Jia D, He P, et al. Influence of calcination temperature of kaolin on the structure and properties of final geopolymer. Mater Lett. 2010;64:2551–2554.
[26] Barbosa VFF, Mackenzie KJD. Thermal behaviour of inorganic geopolymers and composites derived from sodium polysialate. Mater Res Bull. 2003;38:319–331.
[27] Fernández-Jiménez A, Palomo A. Mid-infrared spectroscopic studies of alkali-activated fly ash structure. Microporous Mesoporous Mater. 2005;86:207–214.
[28] Alkan M, Hopa Ç, Yilmaz Z, et al. The effect of alkali concentration and solid/liquid ratio on the hydrothermal synthesis of zeolite NaA from natural kaolinite. Micropor Mesopor Mat. 2005;86:176–184.
[29] Kljajević LM, Nenadović SS, Nenadović MT, et al. Structural and chemical properties of thermally treated geopolymer samples. Ceram Int. 2017;43:6700–6708.
[30] Lee NK, Khalid HR, Lee HK. Synthesis of mesoporous geopolymers containing zeolite phases by a hydrothermal treatment. Micropor Mesopor Mat. 2016;229:22–30.
[31] Li F, Wang X, Yuan T, et al. Lignosulfonate-modified graphene hydrogel with ultrahigh adsorption capacity for Pb(II) removal. J Mater Chem A. 2016;4:11888–11896.
[32] Wang B, Wen J, Sun S, et al. Chemosynthesis and structural characterization of a novel lignin-based biosorbent and its strong adsorption for Pb (II). Ind Crops Prod. 2017;108:72–80.
[33] Bing W, Gao B, Wan Y. Entrapment of ball-milled biochar in Ca-alginate beads for the removal of aqueous Cd(II). J Ind Eng Chem. 2018;61:161–168.
[34] Ge Y, Cui X, Liao C, et al. Facile fabrication of Green geopolymer/alginate hybrid spheres for efficient removal of Cu(II) in water: Batch and column studies. Chem Eng J. 2017;311:126–134.

[35] Deng J, Liu Y, Liu S, et al. Competitive adsorption of Pb(II), Cd(II) and Cu(II) onto chitosan-pyromellitic dianhydride modified biochar. J Colloid Interface Sci. 2017;506:355–364.
[36] An F, Gao B, Dai X, et al. Efficient removal of heavy metal ions from aqueous solution using salicylic acid type chelate adsorbent. J Hazard Mater. 2011;192:956–962.
[37] Ministry of Health of the People's Republic of China. Standards for drinking water quality (GB 5749-2006). Beijing: Standards Press of China; 2006.
[38] Ministry of Ecology and Environment of the People's Republic of China. Integrated wastewater discharge standard (GB 8978-1996). Beijing: Standards Press of China; 1996.
[39] Giles CH, Smith D, Huitson A. A general treatment and classification of the solute adsorption isotherm. I. theoretical. J Colloid Interf Sci. 1974;477:66–778.
[40] Tang Q, Wang K, Yaseen M, et al. Synthesis of highly efficient porous inorganic polymer microspheres for the adsorptive removal of Pb2+ from wastewater. J Clean Prod. 2018;193:351–362.
[41] Luukkonen T, Sarkkinen M, Kemppainen K, et al. Metakaolin geopolymer characterization and application for ammonium removal from model solutions and landfill leachate. Appl Clay Sci. 2016;119:266–276.
[42] Kara İ, Yilmazer D, Akar ST. Metakaolin based geopolymer as an effective adsorbent for adsorption of zinc(II) and nickel(II) ions from aqueous solutions. Appl Clay Sci. 2017;139:54–63.